



## Journal of Advanced Research in Applied Mechanics

Journal homepage:  
[https://semarakilmu.com.my/journals/index.php/appl\\_mech/index](https://semarakilmu.com.my/journals/index.php/appl_mech/index)  
ISSN: 2289-7895



# Wear Scar Characteristics of Thermal Power Plant Waste Reinforced Nickel Matrix Composite Coatings

Intan Sharhida Othman<sup>1,\*</sup>, Rose Farahiyah Munawar<sup>1</sup>, Liew Pay Jun<sup>1</sup>, Jeefferie Abd Razak<sup>1</sup>, Syahrul Azwan Sundi<sup>1</sup>, Mohd Rody Mohamad Zin<sup>2</sup>, Shahira Liza Kamis<sup>3</sup>, Qumrul Ahsan<sup>4</sup>

<sup>1</sup> Fakulti Teknologi dan Kejuruteraan Industri dan Pembuatan, Universiti Teknikal Malaysia Melaka, Hang Tuah Jaya, 76100 Durian Tunggal, Melaka, Malaysia

<sup>2</sup> Fakulti Teknologi dan Kejuruteraan Mekanikal, Universiti Teknikal Malaysia Melaka, Hang Tuah Jaya, 76100 Durian Tunggal, Melaka, Malaysia

<sup>3</sup> Malaysian- Japan International Institute of Technology, Universiti Teknologi Malaysia, Jalan Sultan Yahya Petra, Kampung Datuk Keramat, 54100 Kuala Lumpur, Malaysia

<sup>4</sup> University of Asia Pacific, 74/A, Green Road, Farmgate, Dhaka-1205, Bangladesh

### ARTICLE INFO

#### Article history:

Received 3 August 2023

Received in revised form 5 October 2023

Accepted 21 October 2023

Available online 5 January 2024

#### Keywords:

Nickel; fly ash; composite coating; wear

### ABSTRACT

This research delves into the distinct wear scar properties exhibited by pure nickel and nickel composite coatings with varying concentrations of fly ash when sliding against a stainless steel ball on an aluminium alloy 6061 (AA6061) substrate. The composite coatings were formulated from a modified nickel Watt's bath using an electrodeposition technique, involving a 1-hour process at 40°C and a current density of 5 A/dm<sup>2</sup>. Through experimentation utilizing a high-frequency reciprocating rig (HFRR) tester, the resulting composite coatings underwent assessment, capturing the features of the scar surfaces. Notably, the Ni-FA (nickel-fly ash) composite coating, comprising 90 g/l of fly ash, demonstrated notably enhanced wear resistance in contrast to both the pure nickel coating and the Ni-FA composite coatings with lower fly ash concentrations. The disparities in morphology between the pure nickel and Ni-FA composite coatings were discernible through scanning electron microscopy, energy-dispersive X-ray spectroscopy (EDS), and analysis of surface roughness on the wear scars. These distinctions can be attributed to the varying impacts of fly ash concentration on the wear scar characteristics.

## 1. Introduction

Aluminum and its alloys are widely favored materials across a range of technological applications, including marine, automotive, and aerospace industries. This preference stems from their impressive combination of high strength-to-density ratio, exceptional workability, corrosion resistance, appealing aesthetics, and recyclability [1-4]. Nonetheless, these alloys exhibit inherent surface limitations, including low hardness, diminished wear resistance, and vulnerability to degradation at elevated temperatures [5, 6]. To address these shortcomings and bolster surface characteristics, the

\* Corresponding author.

E-mail address: [intan\\_sharhida@utem.edu.my](mailto:intan_sharhida@utem.edu.my)

<https://doi.org/10.37934/aram.112.1.2131>

integration of nickel composite coatings with aluminum and its alloys has been introduced. This initiative seeks to elevate the surface attributes of these alloys. Notably, study by Pancreciosus *et al.*, [7] underscore that composite coatings resulting from the electrodeposition process display remarkable surface properties, enhanced corrosion resistance, and enhanced wear resistance.

A recent advancement involves the electrodeposition of nickel-based composite coatings wherein diverse ceramic particles like SiC [8-10], SiO<sub>2</sub> [11], TiO<sub>2</sub> [12], and Al<sub>2</sub>O<sub>3</sub> [13] are co-deposited within the nickel matrix. This innovation has been pursued to enhance the mechanical, corrosion, and tribological attributes of the coatings. Collectively, these investigations underscore the critical impact of factors such as the nature, dimensions, concentration, and dispersion of the co-deposited ceramic particles within the metal matrix, as they substantially dictate the properties of the resulting composite coatings. Nevertheless, the widespread implementation of these ceramic particles is hindered by their associated costs.

As an alternative approach, it is prudent to consider the adoption of cost-effective or recycled reinforcement materials to effectively mitigate the expense associated with composite coatings. Fly ash, a finely textured residue resulting from coal combustion in power generation plants, represents a readily available global resource that has posed waste disposal challenges [14]. This fly ash exhibits promise as a potential ceramic reinforcement component for the advancement of metal matrix composites (MMCs), as several studies have been conducted to enhance the mechanical, tribological, and corrosion attributes of these composites. Notably, research by Dinaharan *et al.*, [15] and Marin *et al.*, [16] affirms that fly ash particles, rich in SiO<sub>2</sub> and Al<sub>2</sub>O<sub>3</sub> content, hold potential as cost-effective reinforcing agents, capable of elevating wear resistance and microhardness while concurrently reducing composite material density.

Hence, the primary objective of this study was to investigate the incorporation of fly ash into a nickel matrix composite coating. The research focused on evaluating the impact of different fly ash concentrations on crucial aspects such as surface morphology, surface roughness, and the characteristics of wear scars within the composite coatings.

## 2. Methodology

The AA6061 aluminum alloy substrate, with dimensions of 40 x 30 x 3 mm, underwent a grinding procedure using silicon carbide papers of varying grit sizes, namely 180, 600, 800, and 1200. Subsequently, the substrates underwent a meticulous cleaning protocol that involved ethanol, followed by immersion in a 10 wt.% sodium hydroxide (NaOH) solution for 10 seconds. Following this, they were immersed in a 50 vol.% nitric acid (HNO<sub>3</sub>) solution for 20 seconds. The zincating process was carried out by vertically immersing the thoroughly pre-cleaned substrate into a small glass beaker containing a zincating solution. This immersion lasted for 5 minutes at room temperature. The zincating solution comprised zinc oxide (100 g/l), sodium hydroxide (525 g/l), ferric chloride (1 g/l), and potassium sodium tartrate (9.8 g/l). Stringent rinsing of the samples followed each step to prevent any potential cross-contamination between successive baths.

The pertinent chemical composition and operational parameters for the electrodeposition of the Ni-FA composite coating onto the AA6061 substrate were summarized and are presented in Table 1. The fly ash particles, obtained as a by-product from the Manjung Power Plant in Perak, were sourced from YTL Sdn. Bhd (M). To prepare the fly ash, a ball milling process was conducted for a duration of 2 hours. Figure 1 illustrates the schematic diagram depicting the electrodeposition process of the composite coating.

**Table 1**  
 Composition of modified nickel Watt's bath solution and its operating condition

Composition	Concentration (g/l)
Nickel sulphate hexahydrate	200
Nickel chloride	20
Boric Acid	30
Sodium citrate	30
Operating condition	
Temperature (°C)	40
Deposition time (min)	60
Current density (A/dm <sup>2</sup> )	5
Concentration of fly ash (g/l)	0, 10, 50, 90

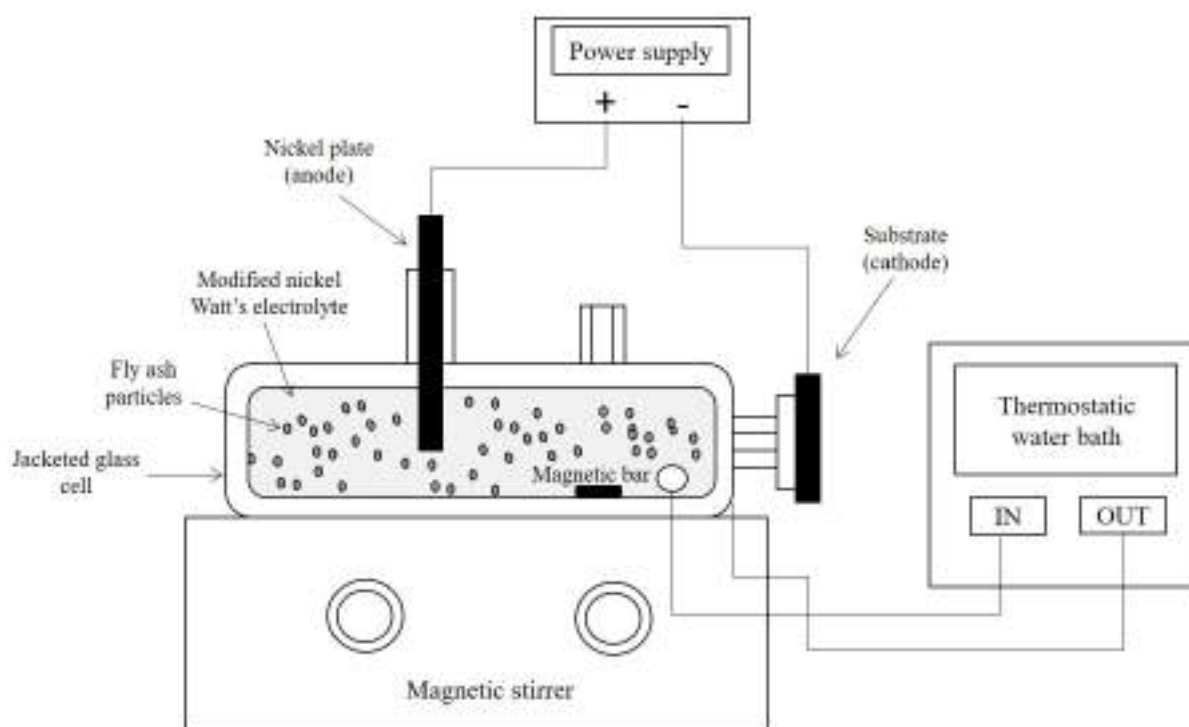


**Fig. 1.** Schematic representation of the electrodeposition procedure

For the purpose of characterization, an in-depth analysis of fly ash particles was conducted using scanning electron microscopy (SEM) and energy dispersive X-ray spectroscopy (EDS) techniques. The surface morphology of both the pure nickel and Ni-FA composite coatings was examined through SEM. To assess the wear performance of the composite coatings, a high-frequency reciprocating rig (HFRR) was employed. This involved subjecting the samples to a 6 mm diameter stainless steel ball with a hardness of 60 HRC. The ball was reciprocated against the samples under a constant 10 N load and at a frequency of 5 Hz. The sliding duration was set to 0.5 hours, with a stroke length of 2 mm. Testing was conducted at room temperature, and a fresh stainless steel ball was utilized for each testing cycle. Subsequently, the resulting wear scars were subjected to analysis using SEM, EDS, and a surface profilometer.

### 3. Results

#### 3.1 Characterization of Fly Ash Particles

According to Figure 2, the point ID on SEM-EDX demonstrates that the mass (%) of elements in each spherical form of fly ash particles varies. This is because fly ash particles include a variety of oxides that are mixed together. Because FA particles are made up of various oxide compositions, the maximum mass at each site is oxide, whereas the lowest mass is sodium (Na).

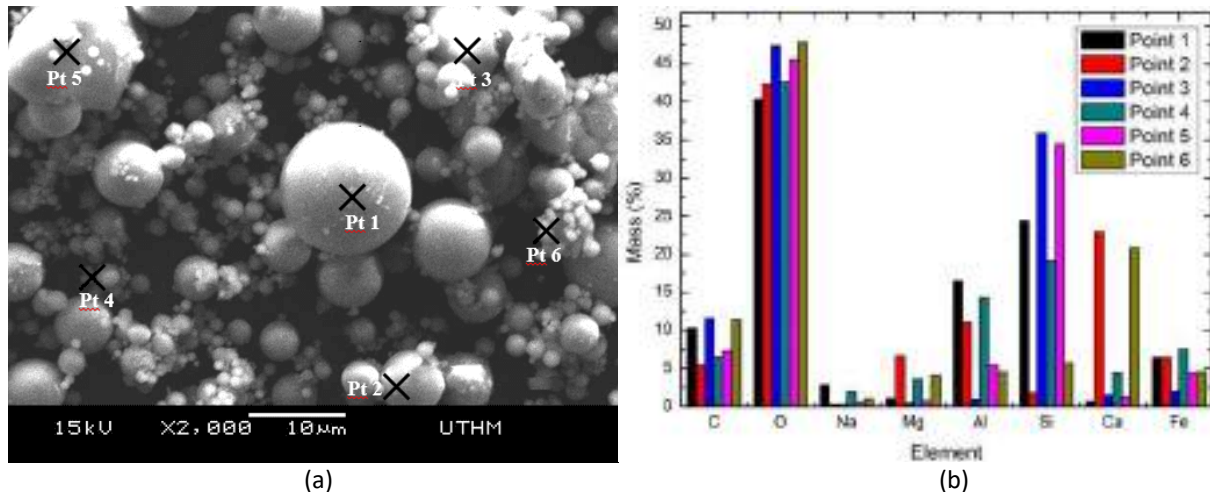


Fig. 2. (a) SEM picture and (b) EDX element mass bar chart for fly ash particles

#### 3.2 Surface Topography of Pure Nickel and Ni-FA Composite Coatings

To assess the successful application of pure nickel and Ni-FA composite coatings onto the substrate, a 3D surface profile analysis was conducted on the coated surface (Figure 3). The depth profile analysis along the horizontal axis is presented in this figure. The uniform deposition of pure nickel onto the substrate is demonstrated in Figure 3(a). However, incorporating fly ash particles at different concentrations into the electrolyte brings about substantial changes in the surface topography of the Ni-FA composite coatings, as depicted in Figure 3(b-d). Notably, the introduction of 10 g/l of fly ash particles into the electrolyte results in a smoothly coated surface with only a few aggregated regions (Figure 3(b)).

The surfaces that underwent coating exhibited increased roughness and more pronounced aggregations when subjected to an electrolyte containing 50 and 90 g/l of fly ash particles (Figure 3 (c & d)). Contrary to initial assumptions, the aggregates depicted in Figure 4 are not fly ash particles, as confirmed by EDS line analysis; instead, they represent the nickel matrix enveloping embedded fly ash particles. The heightened surface roughness of the composite coatings contributes to the development of a nodular structure in the Ni-FA composite coatings, particularly at higher fly ash concentrations.

The composite coatings' aggregation might arise from the suppression of nickel grain enlargement during deposition due to the incorporation of fly ash particles into the matrix. This alteration in crystal growth leads to the formation of finer nickel grains. This finding finds support in the work of Panagopoulos and Georgiou [17], who identified that fly ash particles remained within the nickel matrix, impeding the growth of nickel grains. The microstructural alterations seen in this work support the concepts of Spanou *et al.*, [18], who proposed that the loading of oxide particles in the electrolyte leads in textural changes similar to those reported in pure nickel deposits.

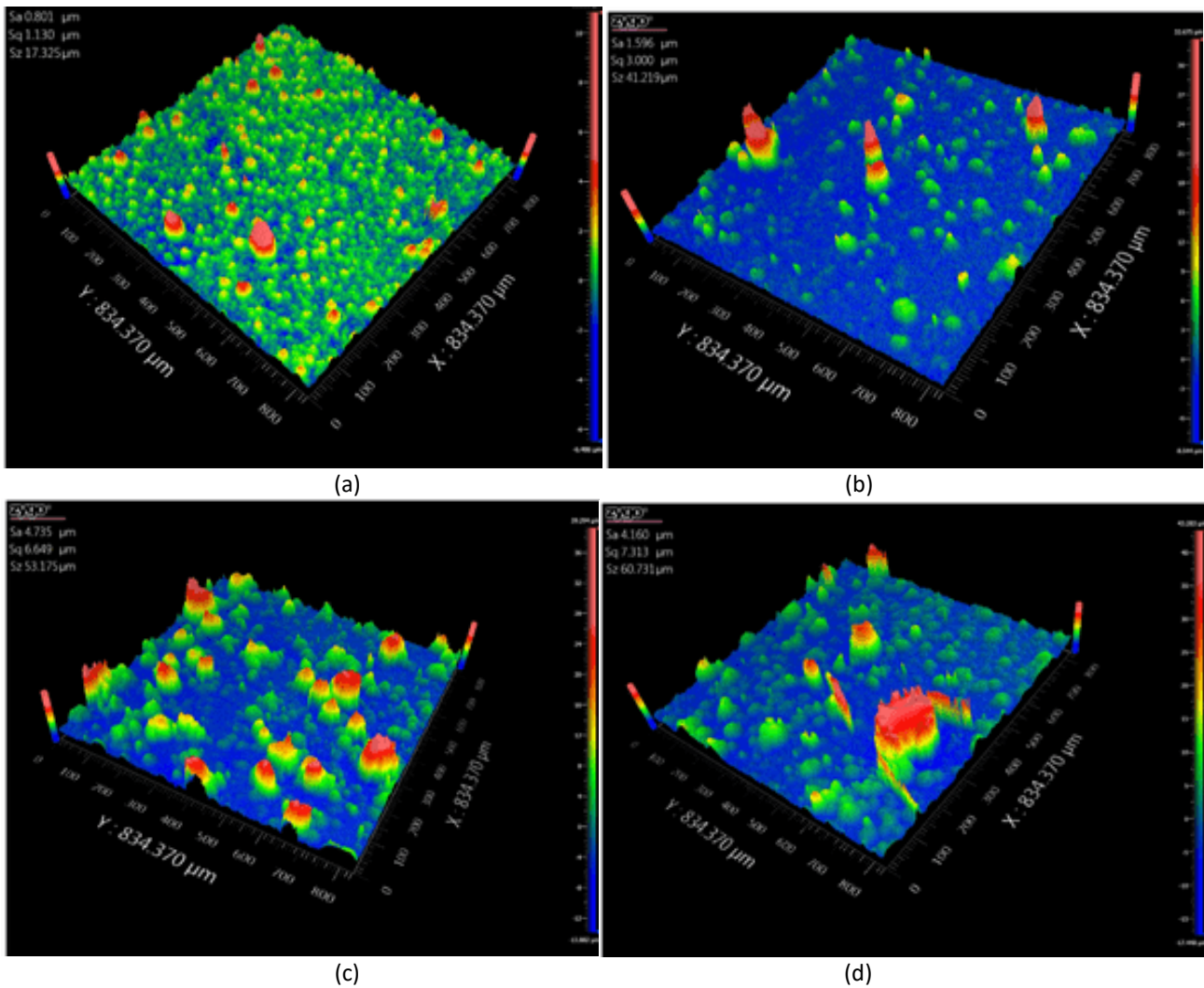


**Fig. 3.** Surface morphology profiles of (a) pure nickel and Ni-FA composite coatings at varied concentration levels (b) 10 (c) 50 and (d) 90 g/l

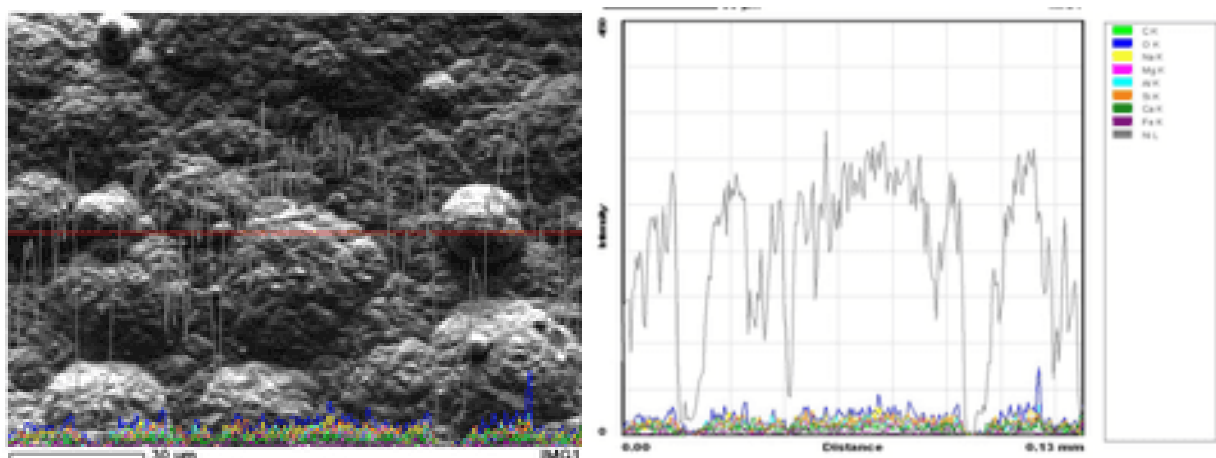


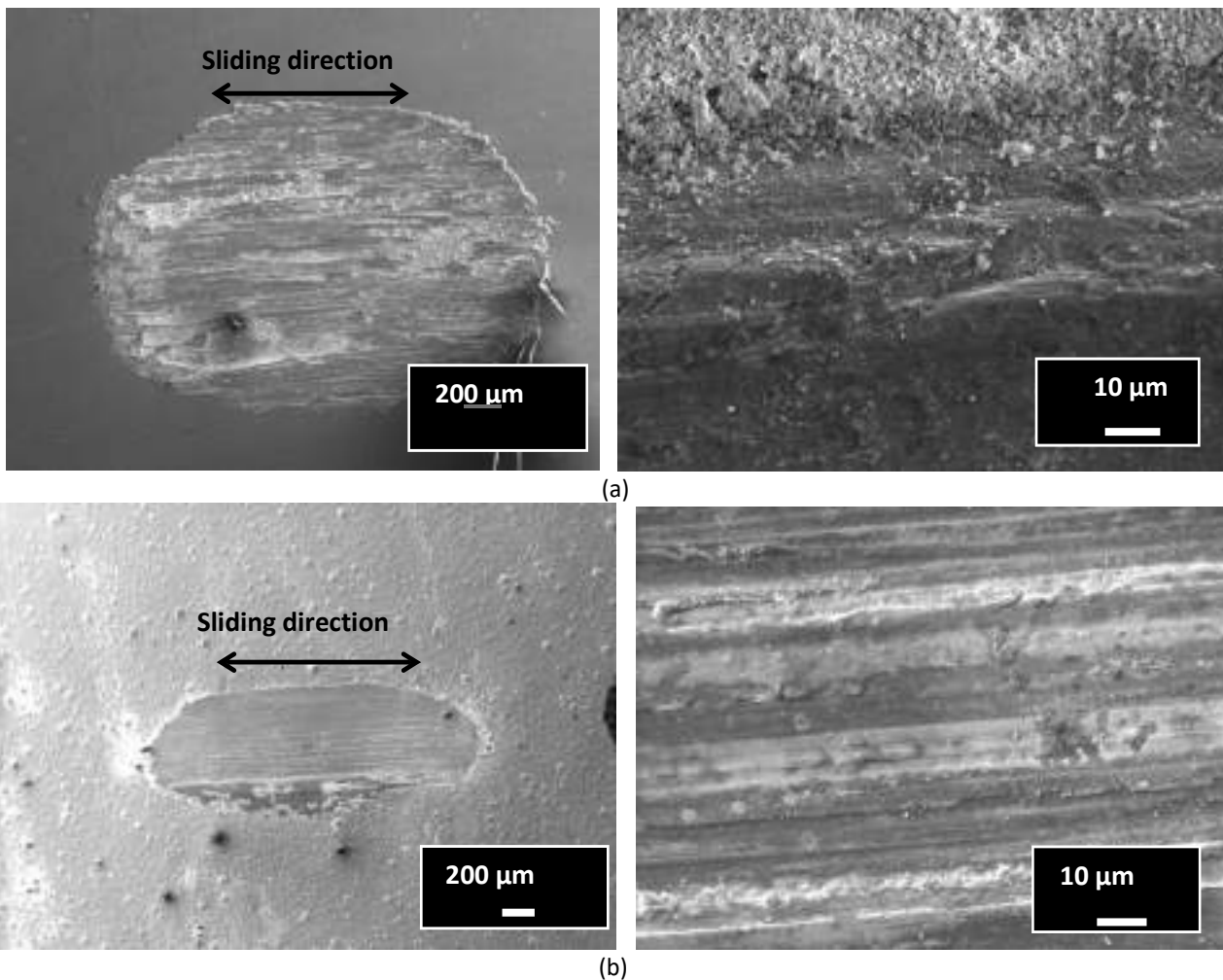
**Fig. 4.** EDX line analysis of a Ni-FA composite coating at a concentration of 90 g/l fly ash

### 3.3 Tribological Properties of Pure Nickel and Ni-FA Composite Coatings

The investigation focused on the tribological properties of both pure nickel coatings and composite Ni-FA coatings through the analysis of wear scars generated during wear testing. The

utilization of scanning electron microscopy (SEM) aided in understanding the wear mechanisms occurring within Ni-FA composite coatings containing varying fly ash contents, following their interaction with a steel ball. The wear scars, as depicted in Figure 5, displayed distinct abrasive grooves predominantly oriented parallel to the sliding direction. Notably, the uncoated substrate suffered significant damage, primarily due to direct contact with the steel ball, consequently exacerbating wear (Figure 5 (a)). This outcome could be attributed to the relatively low hardness of the AA6061 substrate. Conversely, Figure 5 (c-e) illustrated that the incorporation of fly ash particles into the nickel matrix during co-deposition led to an enhancement of worn-out regions on both the AA6061 substrate and pure nickel coating. As suggested by Tamilrasan *et al.*, [19], these worn patches manifested as longitudinal furrows and small grooves aligned with the steel ball's sliding motion.

Notably, the wear characteristics of Ni-FA composite coatings displayed distinctions when compared to the uncoated AA6061 and pure nickel coating samples. A novel wear feature was observed in Ni-FA composite coatings, suggesting potential tribochemical interactions during the wear process. Evident in the wear scar periphery was the occurrence of material transfer, forming spherical entities. This material transfer likely comprised fractured fly ash particles that became entrapped within the sliding interface, embedding themselves in the stainless steel counterface, with the remainder aggregating at the wear scar's edge. Particularly in the Ni-FA composite coating with a fly ash content of 90 g/l, the spherical nature of the robust fly ash particles was more pronounced. This observation aligned with findings by Moorthy *et al.*, [20] who posited that such spherical fly ash particles enhance load-bearing capacity and provide effective matrix alloy protection during dry sliding wear, functioning as a self-lubricating element.



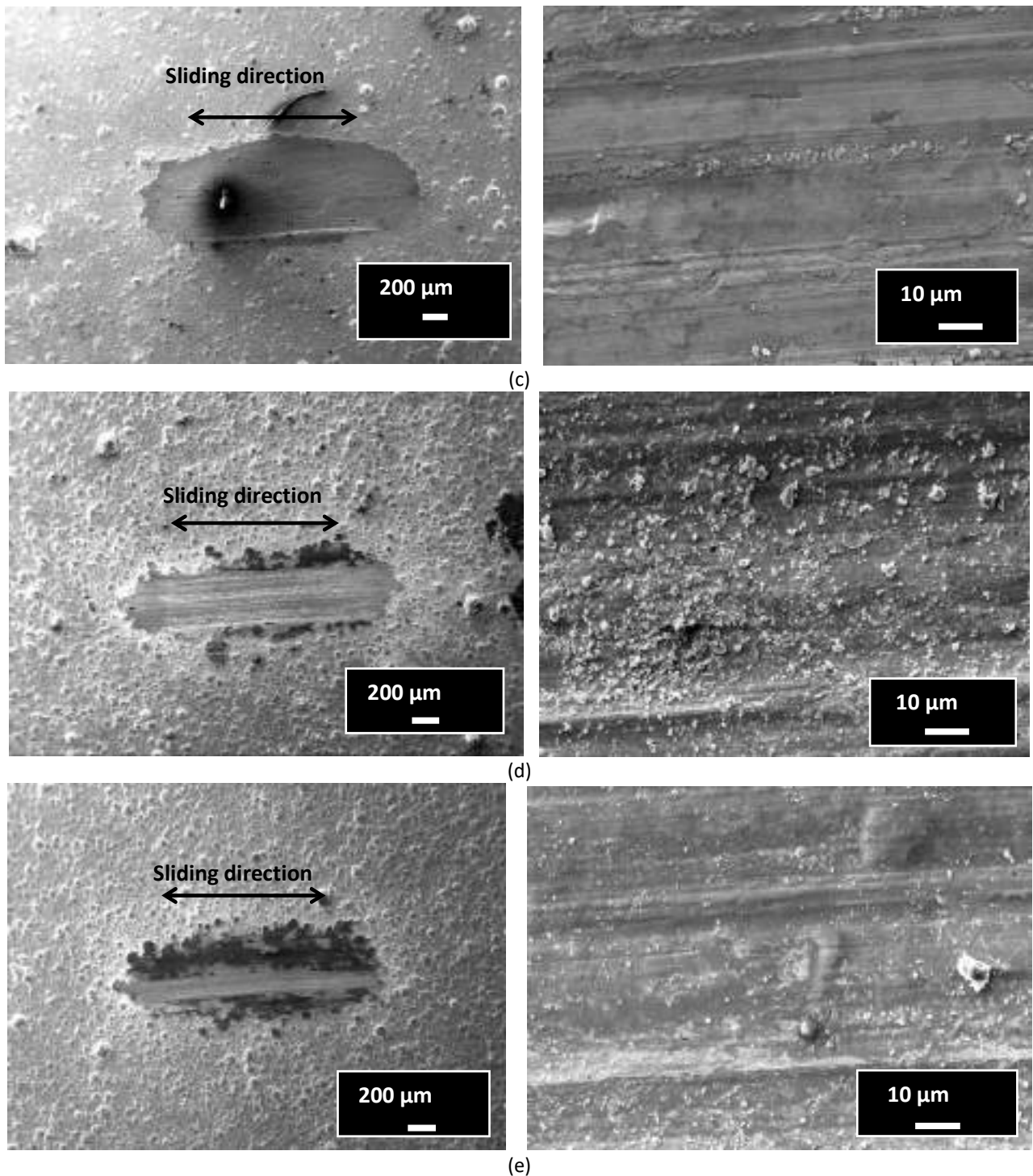


**Fig. 5.** Surface characteristics of the wear track are observed for (a) Untreated AA6061 surface (b) surface coated with pure nickel, and composite Ni-FA coating with different concentration of (c) 10 (d) 50 and (e) 90 g/l

Owing to the irregular characteristics of the wear scar, which hinder the accurate calculation of worn volume, the dimensions of the wear scar shown in Figure 5 were utilized to quantify the extent of wear damage. Notably distinct are the dimensions of wear scars on the AA6061 substrate, pure nickel coating, and Ni-FA composite coatings (Figure 6). The AA6061 substrate has the largest and longest wear scar, indicating poor wear resistance. On the other hand, the width and length of the wear scar were significantly diminished when the substrate underwent electrodeposition with pure

nickel or Ni-FA composite coatings. However, no significant variation in the length of the wear scar was identified between pure nickel and Ni-FA composite coatings. The width of the wear scar narrows as the fly ash concentration increases from 10 to 90 g/l. It has been proposed that the breadth and depth of the worn region provide information about wear resistance [21].

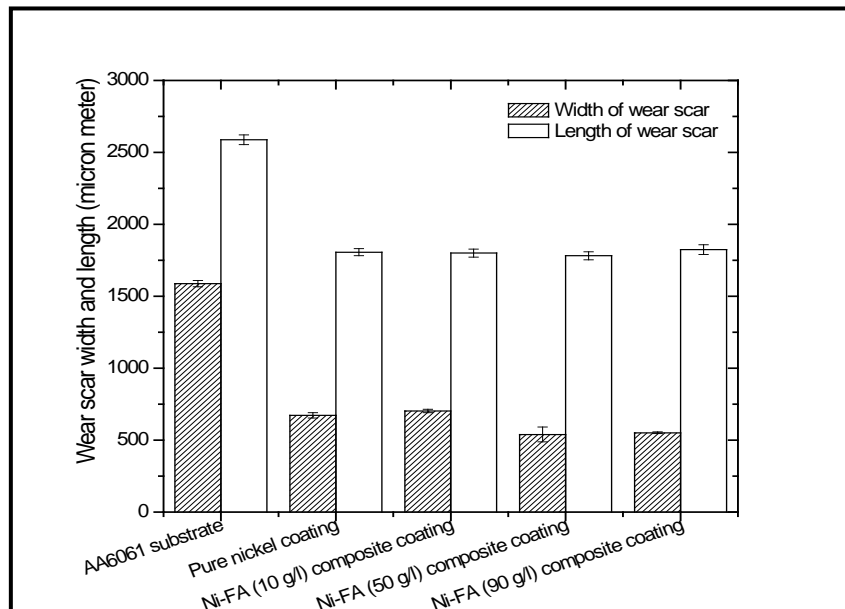
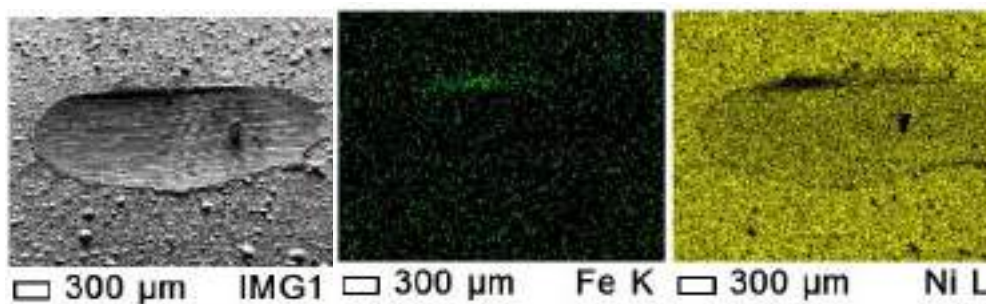


**Fig. 6.** Width and length of wear scars on AA6061 substrate, pure nickel and Ni-FA composite coatings

As depicted in Figures 5(c-e), at elevated levels of fly ash content within the nickel matrix, the surface material is observed to be displaced towards the periphery of the wear track. This observation aligns with the outcomes of the EDS analysis, which not only verified the presence of wear debris expelled to the scar's edge (Figure 7) but also highlighted that Ni-FA (90 g/l) composite coating exhibited the highest iron composition. This elevated iron content is believed to have been transferred from the steel ball to the coating during the wear testing. It's plausible that these findings can be attributed to the greater microhardness of the Ni-FA (90 g/l) composite coating in comparison to the steel ball. Furthermore, the EDS elemental mapping results indicate a progressive increase in iron content from 0.67% at 10 g/l fly ash to 7.18% at 90 g/l fly ash (Table 2). The scar exhibits the characteristic appearance of ploughing wear. Iron on the wear track indicates material transfer from the steel counter body to the coatings. The presence of a significant amount of oxygen on the wear tracks suggests that oxidation occurred during the wear of Ni-FA composite coatings against steel.



(a)



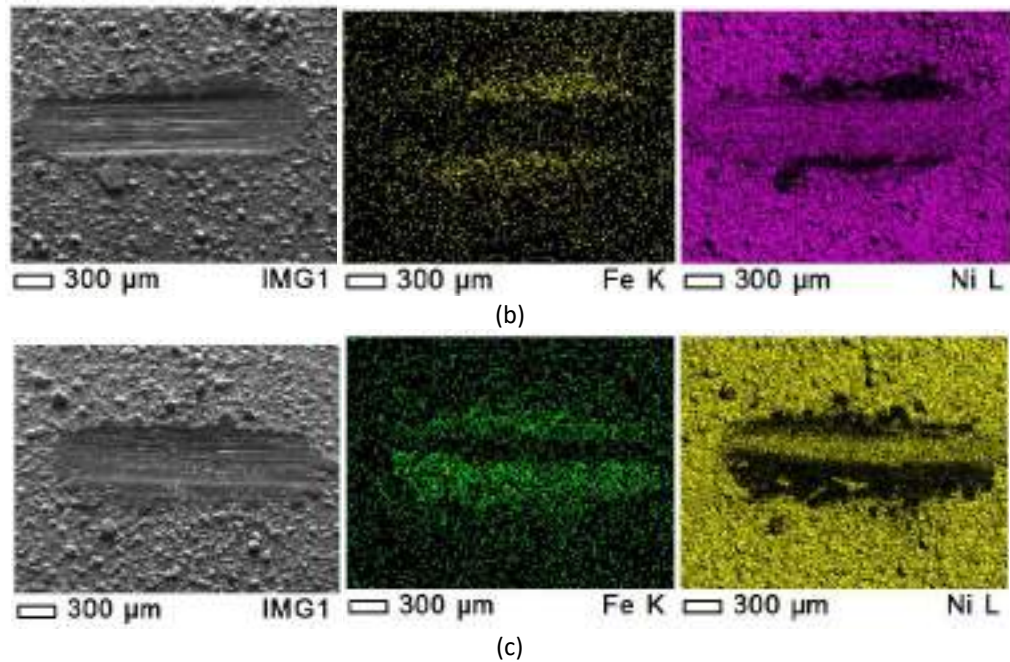


**Fig. 7.** Elemental mapping using EDS for Ni-FA composite coatings with different fly ash contents: (a) 10 (b) 50 and (c) 90 g/l

**Table 2**

EDS elemental mapping of Ni-FA composite coatings at varied fly ash concentration

Element (mass %)	Fly ash concentration		
	10 g/l	50 g/l	90 g/l
C	6.54	2.56	2.47
O	5.77	7.73	6.95
Fe	0.67	4.79	7.18
Ni	84.42	82.21	81.32

#### 4. Conclusions

On an AA6061 substrate, pure nickel coatings and Ni-FA composite coatings with varying fly ash concentrations were successfully electrodeposited. Coating features such as surface morphology and tribological properties were investigated. The following are some of the study's most notable findings:

- i. As the fly ash concentration increases from 10 to 90 g/l, the surface roughness increases from 1.04 to 5.43 m
- ii. At 90 g/l of fly ash, the width and length of the composite coating's wear scars show a significant improvement
- iii. The wear groove exhibited enhancement in the Ni-FA composite coating at a concentration of 90 g/l
- iv. The increased tribological properties of the Ni-FA (90 g/l) composite coating is attributed to the greater surface roughness and tougher surface of coatings produced with a high fly ash concentration

## Acknowledgement

This research was funded by a grant from Universiti Teknikal Malaysia Melaka (Short Term Research (PJP) Grant PJP/2022/FKP/S01875).

## References

- [1] Sharifalhosseini, Zahra, and Ali Davoodi. "Uniform nucleation of zincate layer through the optimized etching process to prevent failure in electroless plating on 2024 aluminum alloy." *Engineering Failure Analysis* 124 (2021): 105326. <https://doi.org/10.1016/j.engfailanal.2021.105326>
- [2] Yan, Ping, Jianxin Zou, Conglin Zhang, and Thierry Grosdidier. "Surface modifications of a cold rolled 2024 Al alloy by high current pulsed electron beams." *Applied Surface Science* 504 (2020): 144382. <https://doi.org/10.1016/j.apsusc.2019.144382>
- [3] Makoto, H. I. N. O., Koji Murakami, Yutaka Mitooka, Ken Muraoka, and Teruto Kanadani. "Effects of zincate treatment on adhesion of electroless Ni-P coating onto various aluminum alloys." *Transactions of Nonferrous Metals Society of China* 19, no. 4 (2009): 814-818. [https://doi.org/10.1016/S1003-6326\(08\)60356-8](https://doi.org/10.1016/S1003-6326(08)60356-8)
- [4] Aal, A. Abdel. "Hard and corrosion resistant nanocomposite coating for Al alloy." *Materials Science and Engineering: A* 474, no. 1-2 (2008): 181-187. <https://doi.org/10.1016/j.msea.2007.04.058>
- [5] Bocking, C., and A. Reynolds. "Mechanism of adhesion failure of anodised coatings on 7075 aluminium alloy." *Transactions of the IMF* 89, no. 6 (2011): 298-302. <https://doi.org/10.1179/174591911X13173054200817>
- [6] Visser, P. "Novel totally chrome free corrosion inhibiting coating technology for protection of aluminium alloys." *Transactions of the IMF* 89, no. 6 (2011): 291-294. <https://doi.org/10.1179/174591911X13172025236839>
- [7] Pancrecius, Jerin K., P. S. Gopika, P. Suja, Sarah Bill Ulaeto, E. Bhoje Gowd, and T. P. D. Rajan. "Role of layered double hydroxide in enhancing wear and corrosion performance of self-lubricating hydrophobic Ni-B composite coatings on aluminium alloy." *Colloids and Surfaces A: Physicochemical and Engineering Aspects* 634 (2022): 128017. <https://doi.org/10.1016/j.colsurfa.2021.128017>
- [8] Huang, Pao-Chang, Kung-Hsu Hou, Jia-Jun Hong, Meng-Hung Lin, and Gao-Liang Wang. "Study of fabrication and wear properties of Ni-SiC composite coatings on A356 aluminum alloy." *Wear* 477 (2021): 203772. <https://doi.org/10.1016/j.wear.2021.203772>
- [9] Franco, M., W. Sha, G. Aldic, S. Malinov, and Hüseyin Çimenoglu. "Effect of reinforcement and heat treatment on elevated temperature sliding of electroless Ni-P/SiC composite coatings." *Tribology international* 97 (2016): 265-271. <https://doi.org/10.1016/j.triboint.2016.01.047>
- [10] Mosisili, Mankgoana, Velaphi Msomi, and Sipokazi Mabuwa. "SiC, titanium, nickel, and ferric acid reinforcement materials to enhance mechanical properties in aluminium alloys: A critical review." *Materials Today: Proceedings* 56 (2022): 2268-2273. <https://doi.org/10.1016/j.matpr.2021.11.606>
- [11] Islam, Mohammad, Muhammad Rizwan Azhar, Narjes Fredj, T. David Burleigh, Olamilekan R. Oloyede, Abdulhakim A. Almajid, and S. Ismat Shah. "Influence of SiO<sub>2</sub> nanoparticles on hardness and corrosion resistance of electroless Ni-P coatings." *Surface and Coatings Technology* 261 (2015): 141-148. <https://doi.org/10.1016/j.surfcoat.2014.11.044>
- [12] Birlik, Isil, N. Funda Ak Azem, Mustafa Toparli, Erdal Celik, Tulay Koc Delice, Sidika Yildirim, Onur Bardakcioglu, and Tuncay Dikici. "Preparation and characterization of ni-TiO<sub>2</sub> nanocomposite coatings Produced by electrodeposition Technique." *Frontiers in Materials* 3 (2016): 46. <https://doi.org/10.3389/fmats.2016.00046>
- [13] Karthikeyan, S., and B. Ramamoorthy. "Effect of reducing agent and nano Al<sub>2</sub>O<sub>3</sub> particles on the properties of electroless Ni-P coating." *Applied Surface Science* 307 (2014): 654-660. <https://doi.org/10.1016/j.apsusc.2014.04.092>
- [14] Khairul Nizar, Ismail, AM Mustafa Al Bakri, Rafiza Abd Razak, Hussin Kamarudin, Alida Abdullah, and Yahya Zarina. "Study on physical and chemical properties of fly ash from different area in Malaysia." *Key Engineering Materials* 594 (2014): 985-989. <https://doi.org/10.4028/www.scientific.net/KEM.594-595.985>
- [15] Dinaharan, I., S. Karpagarajan, R. Palanivel, and J. David Raja Selvam. "Microstructure and sliding wear behavior of fly ash reinforced dual phase brass surface composites synthesized through friction stir processing." *Materials Chemistry and Physics* 263 (2021): 124430. <https://doi.org/10.1016/j.matchemphys.2021.124430>
- [16] Marin, Elia, Maria Lekka, Francesco Andreatta, Lorenzo Fedrizzi, Grigorios Itskos, Aggeliki Moutsatsou, Nikolaos Koukouzas, and Niki Kouloumbi. "Electrochemical study of Aluminum-Fly Ash composites obtained by powder metallurgy." *Materials Characterization* 69 (2012): 16-30. <https://doi.org/10.1016/j.matchar.2012.04.004>
- [17] Panagopoulos, C. N., and E. P. Georgiou. "Surface mechanical behaviour of composite Ni-P-fly ash/zincate coated aluminium alloy." *Applied Surface Science* 255, no. 13-14 (2009): 6499-6503. <https://doi.org/10.1016/j.apsusc.2009.02.026>

- [18] Spanou, S., E. A. Pavlatou, and N. Spyrellis. "Ni/nano-TiO<sub>2</sub> composite electrodeposits: textural and structural modifications." *Electrochimica Acta* 54, no. 9 (2009): 2547-2555. <https://doi.org/10.1016/j.electacta.2008.06.068>
- [19] Tamilarasan, T. R., R. Rajendran, U. Sanjith, G. Rajagopal, and J. Sudagar. "Wear and scratch behaviour of electroless Ni-P-nano-TiO<sub>2</sub>: Effect of surfactants." *Wear* 346 (2016): 148-157. <https://doi.org/10.1016/j.wear.2015.11.015>
- [20] Moorthy, A. Anandha, N. Natarajan, P. K. Palani, and M. Suresh. "Study on tribological characteristics of self-lubricating aa2218–fly ash–white graphite composites." *Int J Eng Technol* 5 (2013): 4193-4198.
- [21] Gyawali, Gobinda, Khagendra Tripathi, Bhupendra Joshi, and Soo Wahn Lee. "Mechanical and tribological properties of Ni-W-TiB<sub>2</sub> composite coatings." *Journal of Alloys and Compounds* 721 (2017): 757-763. <https://doi.org/10.1016/j.jallcom.2017.06.044>